Visualizing Photochemical Dynamics in Solution through Picosecond X-Ray Scattering

Richard Neutze,[1,*] Remco Wouts,[2] Simone Techert,[3] Jan Davidsson,[4] Menhard Kocsis,[3] Adam Kirrander,[2] Friedrich Schotte,[3] and Michael Wulff[3,†]

[1]*Department of Molecular Biotechnology, Chalmers University of Technology, P.O. Box 462, SE 40530 Göteborg, Sweden*
[2]*Department of Biochemistry, Biomedical Centre, Box 576, Uppsala University, S-75123 Uppsala, Sweden*
[3]*European Synchrotron Radiation Facility, BP 220, Grenoble Cedex 38043, France*
[4]*Department of Physical Chemistry, Box 532, Uppsala University, S-75121 Uppsala, Sweden*

(Received 30 March 2001; published 23 October 2001)

A photoexcited state of molecular iodine in solution is observed using diffuse x-ray scattering at a synchrotron source. The measured changes in the diffuse scattering profile were consistent with earlier models of iodine's photodissociation and geminate recombination reaction, for which the recombined A/A' state has a 0.4 Å greater interatomic spacing than the resting state and has a lifetime of 500 ps in CH_2Cl_2. This technique should find application in the study of increasingly complicated photochemical systems which undergo structural rearrangements following rapid photolysis.

DOI: 10.1103/PhysRevLett.87.195508 PACS numbers: 61.10.Eq, 78.47.+p, 82.53.Eb

Ultrafast spectroscopy has enabled electronic and vibrational transitions to be probed with a temporal resolution of femtoseconds [1]. On these time scales the fastest photochemical events, such as photoisomerization or the breakage and formation of chemical bonds, can be followed. A detailed knowledge of the energy surfaces of the ground state and all accessible excited species, however, is required when interpreting any spectroscopic signal. This presents severe challenges as the system of study increases in complexity.

Experimental probes using electrons [2–5] or x rays offer a means for imaging motions of atomic nuclei directly. Time-resolved x-ray diffraction studies on macromolecules with nanosecond resolution [6,7], picosecond resolution diffraction studies of surface melting [8,9], and picosecond studies of large amplitude motions of an excited chemical system [10]highlight the experimental possibilities opened up by recent advances in x-ray brilliance at synchrotron sources. Other pulsed x-ray sources have facilitated gas phase [11]and solution phase [12]picosecond x-ray absorption experiments and have enabled the growth of disorder in an organic sample [13], and the melting [14] and reordering of a semiconductor surface [15], to be followed. Since x rays have a wavelength the order of atomic separations, a laser pump, x-ray probe approach offers a direct method for recording ultrafast structural changes from photochemical species in solution.

Solvents have a profound influence on the dynamics of chemical reactions. Following photodissociation, bond formation is enhanced by the trapping of reactive species in a solvent cage [16,17]and electronic and vibrational relaxation of excited species to the ground state is controlled by energy coupling with the surrounding medium [18–22]. Although molecular dynamics calculations have been used to illustrate how ultrafast diffuse x-ray scattering could (in principle) observe solvent caging effects [23], only recently has the peak brightness of pulsed x-ray source technology reached the point that such studies become feasible. Ultrafast diffuse x-ray scattering experiments, however, present a number of challenges which must be overcome: as with picosecond electron scattering from photochemical systems in the gas phase [2–5] there is no crystalline lattice with which to enhance the signal above the background; and scattering from the solvent, which comprises approximately 99.7% of all molecules within the sample, exaggerates signal-to-noise concerns.

In this work we used synchrotron radiation to observe a transient state of molecular iodine in solution following excitation by a femtosecond light pulse. Data were collected at ID09 of the European Synchrotron Radiation Facility. The experiment is illustrated schematically in Fig. 1. Monochromatic ($\lambda = 0.75$ Å) 80 ps full width half maximum x-ray pulses were isolated from a single electron bunch using a mechanical x-ray chopper spinning at 897 Hz [24]. Sample photolysis was achieved using a

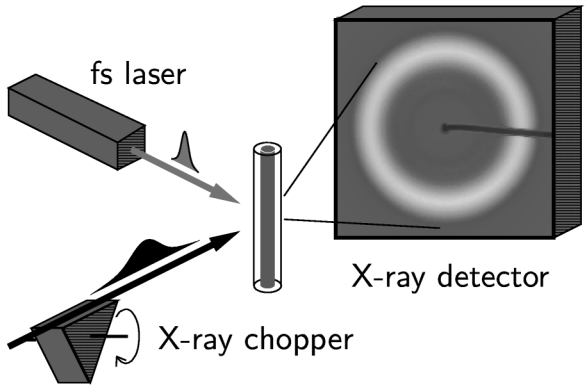

FIG. 1. Schematic illustration of the experimental setup. 80 ps x-ray pulses were isolated from a single electron bunch within the synchrotron ring using a mechanical x-ray chopper. Sample photolysis was achieved using a 100 fs laser mode locked to the clock of the synchrotron. Changes in diffuse x-ray scattering intensities were recorded using an image intensified CCD x-ray camera (Fig. 3a), or using a gas filled detector coupled to a lock-in amplifier (Fig. 4).

femtosecond laser phase locked to the clock of the synchrotron. Electronic jitter between the 80 ps x ray and 100 fs laser pulses was 3 to 5 ps.

Photodissociation and recombination of molecular iodine I_2 in solution, $I_2 + h\nu \rightarrow I^{\cdot} + I^{\cdot} \rightarrow I_2$, were chosen as a prototype system of study. This reaction (Fig. 2) proceeds either through direct excitation to a dissociative energy surface (e.g., $^1\pi_u$) or through excitation to an initially bound state (e.g., B) followed by rapid curve crossing to a dissociative surface [17]. As the two iodine radicals move apart the surrounding solvent responds, absorbing their kinetic energy and forming a solvent cage [16]. Within a few picoseconds, atoms trapped within this cage recombine geminately (i.e., with their original partner) onto either the A, A', or X potential. Those recombining on A or A' undergo solvent induced curve crossing to the X potential prior to vibrational relaxation back to the ground state, and the time scale for this is strongly solvent dependent [19,22]. Atoms which break out of the cage diffuse through the solvent and recombine nongeminately on a slower time scale [25]. Despite the simplicity of this reaction, with the same diatomic being both reactant and product, controversy persisted as to the assignment of time scales for each of the dissociation and recombination steps [17–22]. Its resolution required the explicit consideration of vibrational mode dynamics for the ground state and all transient species sampled over a variety of pump and probe wavelengths [17,21], highlighting the difficulties encountered when building a unique picture from spectroscopic observations alone.

Diffuse x-ray scattering represents a spherical average of scattering contributions from all randomly oriented molecules within the sample. The observed scattering intensity [Eq. (10.3) in [26]] is proportional to

$$I \propto \sum_m \sum_n f_m f_n \frac{\sin Q r_{mn}}{Q r_{mn}}, \qquad (1)$$

where f_m is the atomic scattering factor of the mth atom of the sample, $Q = 4\pi \sin\theta/\lambda$ where 2θ is the angular deflection of the scattered x ray, and r_{mn} is the distance between the mth and nth atom of the sample. When the interatomic distances of a fraction of the sample's molecules are perturbed by photolysis, then the measured x-ray scattering profile is also affected [23]. As such, light induced changes in the diffuse x-ray scattering pattern correlate directly to structural changes in the probed photochemical system.

Figure 3 displays the measured changes in the diffuse x-ray scattering intensities ($\Delta I \equiv$ laser on minus laser off) resulting from the photolysis of a solution of 40 mMol I_2 (>99.5% purity) dissolved in CH_2Cl_2 (proanalysis grade). This solution was pumped through a 300 μm diameter quartz capillary mounted in the x-ray beam, and photolysis was achieved using 25 μJ 100 fs pulses centered at

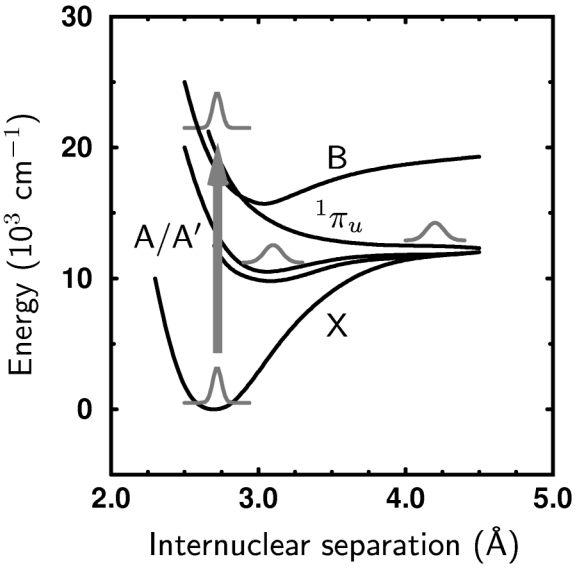

FIG. 2. Schematic illustration of the energy surfaces of molecular iodine. Following photon absorption a repulsive energy surface is reached and the two atoms rapidly move apart. Loss of kinetic energy to the surrounding solvent causes iodine radicals to become trapped, and they may either recombine geminately (with their original partner) or break out of the solvent cage. Recombined iodine can populate the A, A', or X states prior to relaxation back to the ground state.

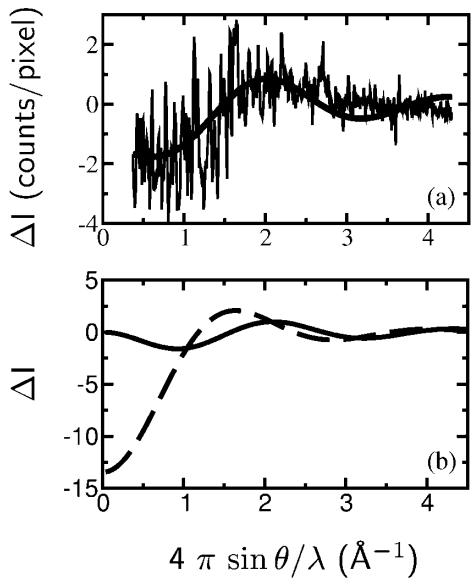

FIG. 3. Changes in the diffuse x-ray scattering intensities. (a) Experimentally measured changes (average photon counts per pixel) resulting from the photolysis of 40 mMol I_2 in CH_2Cl_2. The solid line shows the predicted differences when the photolyzed sample has a population of 25% A/A' (Fig. 2) and 5% escapes the solvent cage. (b) Theoretical models for changes in the diffuse x-ray scattering profile when the ground state is converted into either A or A' states (solid line) or for cage breakout (dashed line). Data were collected using a hybrid filling of the European Synchrotron Radiation Facility [24].

$\lambda = 530$ nm with a focal spot diameter ≈ 100 μm. The timing was set such that sample photolysis occurred on the rising edge of the 80 ps x-ray pulse. Data were integrated for 1000 s on an image-intensified charge-coupled device camera (110 μm/pixel) located 100 mm from the sample. Images were binned into rings using Bresenham's algorithm, were normalized, and were subtracted. Figure 3a shows the raw signal due to photolysis of iodine in solution (laser on minus laser off). An oscillatory behavior in the difference signal was observed, illustrating a decreased x-ray scattering intensity at low angular deflection and a corresponding increase at medium deflection angle. The units of Fig. 3a are the average number of photon counts per pixel within each ring where, for example, 620 pixels contributed to the ring integration at $4\pi \sin\theta/\lambda = 1$.

In modeling ΔI it is convenient to divide Eq. (1) into three summations: that over the two iodine atoms, that over the iodine-solvent cross term, and that due to the solvent molecules alone. Figure 3b gives the theoretically expected changes (incorporating all geometric and polarization corrections) in the x-ray scattering profile following sample photolysis due to the predominant iodine-iodine term. The solid line predicts the change when the A/A' state is populated, whereas the dashed line gives the same prediction following cage breakout. Interatomic distances for a populated X state were modeled as a 0.1 Å Gaussian distribution about a mean of 2.66 Å [27], for the A/A' state as a 0.2 Å distribution about a mean of 3.02 Å [27], and molecules which escaped the solvent cage were taken to assume an infinite atomic separation. These calculations showed negligible dependence on the width of the X and A/A' states. Intensity changes due to the iodine-solvent cross term, as well as the solvent-solvent term, are significantly reduced since $f_{\mathrm{Cl}} \approx f_{\mathrm{I}}/3$ and $f_{\mathrm{C}} \approx f_{\mathrm{I}}/9$ at $\theta = 0$ and both fall off more rapidly with increasing θ. Furthermore, from Eq. (1) it follows that the magnitude of each term and its period of oscillation decrease as the interatomic spacing, r_{mn}, increases. As such a simple model indicates that the maximum contribution of the iodine-solvent cross term is less than 20% of the iodine-iodine term and oscillates more rapidly. This could not be resolved within experimental errors and was not incorporated into the model. With these simplifications, a least squares fit to the experimental data (solid line, Fig. 3a) then estimated that 25% $\pm$ 3% A/A' was populated following photolysis, and 5% $\pm$ 3% escaped the solvent cage. A change in the modeled interatomic spacing of 0.2 Å for the A/A' state was needed to double the variance squared against the filtered signal, and it was not possible to distinguish between molecules which recombined on either of the A, A', or X states. An oscillation at higher deflection angle was not resolved, possibly due to clustering effects at the high concentrations used in this experiment complicating the description of the system. This is further suggested by the fact that the nongeminate yield (15% of the photolyzed sample) was reduced relative to that (40%) determined from the ns bleach of photolyzed I_2 in CH_2Cl_2 [22]. Rapid heating may also induce structural changes in the solvent, although Laue diffraction studies on protein crystals indicate that thermal effects take ~ 1 μs to become significant [6].

Because of the small amplitude of the measured changes in the diffuse x-ray scattering intensities ($\approx 0.1\%$ of the raw signal), their temporal dependence was followed by incorporating a lock-in detection system into the experimental design. A gas filled x-ray detector masked to accept from $4\pi \sin\theta/\lambda = 0.4$ to 1.5 Å^{-1} was used to feed a lock-in amplifier, and an optical chopper both stroboscopically blocked the laser beam at 137 Hz and provided the reference signal for the lock-in amplifier. Figure 4 shows the experimental result measured as a function of the time delay, Δt, between the laser pump and the x-ray probe. In this experiment 20 μJ laser pulses centered at $\lambda = 505$ nm were used to photolyze a liquid jet of 40 mMol I_2 in CH_2Cl_2 emerging from the tip of a 100 μm quartz capillary. Data were averaged over a 60 s interval following a steady rise (due to a 100 s averaging window for the lock-in amplifier) in the output voltage of the lock-in amplifier, and uncertainty bars derive from the standard deviation of the signal plus that (about zero) of the output voltage without photolysis. Within the selected Q domain, the contribution of the A/A' species to the negative signal is maximal and decays exponentially with a time constant of 500 ps [19,22], whereas the signal from the iodine radicals (which recombine nongeminately) contributes a constant offset. Using this model, the temporal dependence of the signal was predicted by convolution [28] with the known x-ray pulse profile and is consistent with the experimental results (Fig. 4, solid line).

By observing both light-induced changes in the diffuse x-ray scattering profile (Fig. 3) and following their variation with time (Fig. 4) our results establish that the peak

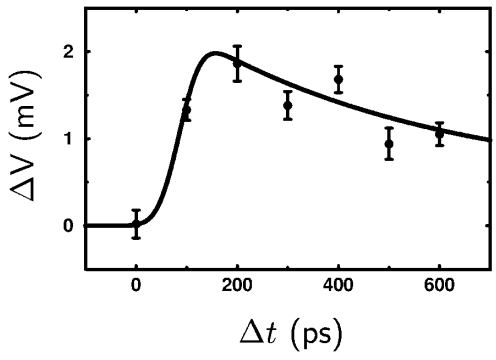

FIG. 4. Temporal dependence of the difference signal due to the photolysis of I_2 in CH_2Cl_2. Each data point records the relative amplitude of the negative peak of Fig. 3a sampled from $Q = 0.4$ Å^{-1} to 1.5 Å^{-1}. The response of the system was predicted (solid line) from the 500 ps lifetime of the A/A' states [19,22] and a constant offset due to cage breakout. Data were collected using a 16-bunch filling of the European Synchrotron Radiation Facility [24].

x-ray brilliance available at a synchrotron source is sufficient to recover a picosecond signal from a transient photochemical species in solution. It is straightforward to increase the x-ray flux at the sample position by relaxing the bandwidth of the x-ray probe at the (relatively minor) cost of decreasing the resolution in Q ($= 4\pi \sin\theta/\lambda$). For example, a bandwidth of 0.014% for the Si_{111} monochromator (used in these experiments) can be increased to a 1.0% bandwidth using multilayer optics or a few percentage points using the full x-ray spectrum of a single-harmonic undulator. In combination with the planned installation of an in-vacuum undulator and upgrades to the x-ray optics, an improvement of approximately 3 orders of magnitude in the number of x-ray photons per pulse to reach the sample appears realistic. In parallel with the use of a tunable high powered ps (or even, in some cases, ns) laser ($\approx$10 mJ/pulse, 10 Hz repetition rate) the overall sensitivity of the experimental technique should be greatly enhanced, allowing more challenging systems to be studied. The temporal resolution may be improved through deconvolution [28], as do existing femtosecond x-ray sources [13,15,29,30]offer promise for similar experiments.

A natural extension of the technique would be to study the structural dynamics of related systems, such as the recombination reaction of photodissociated CH_2I_2 in solution [31]. A more challenging problem might be to follow the light driven vectorial transport of halide ions across a cell membrane (where the sample could be prepared as stacked bilayer) by the chloride pump halorhodopsin [32], which (under certain conditions) also pumps iodide. Other outstanding problems in structural biology, such as the direct visualization of large-scale coherent reaction dynamics in bacterial reaction centers [33], await the availability of extremely brilliant fs x-ray sources [34]. Since the observed changes derive unambiguously from structural rearrangements, the approach developed here should ultimately complement established ultrafast spectroscopy methods.

We thank Savo Bratos, Armin Geis, Janos Hajdu, Hans Pettersson, and Rodolphe Vuilleumier for discussions. This work was supported by the Swedish Natural Science Research Council (NFR), the Swedish Technical Science Research Council (TFR), the Swedish Foundation for Strategic Research (SSF), and the EU-Commission through the Human Potential and BIOTECH Programmes.

*Corresponding author.
Email address: neutze@xray.bmc.uu.se
†Corresponding author.
Email address: wulff@esrf.fr

[1] A. H. Zewail, J. Phys. Chem. A **104**, 5660 (2000).
[2] J. C. Williamson, J. Cao, H. Ihee, H. Frey, and A. H. Zewail, Nature (London) **386**, 159 (1997).
[3] J. Cao, H. Ihee, and A. H. Zewail, Chem. Phys. Lett. **290**, 1 (1998).
[4] J. Cao, H. Ihee, and A. H. Zewail, Proc. Natl. Acad. Sci. U.S.A. **96**, 338 (1999).
[5] H. Ihee, V. A. Lobastov, U. M. Gomez, B. M. Goodson, R. Srinivasan, C. Y. Ruan, and A. H. Zewail, Science **291**, 458 (2001).
[6] V. Srajer *et al.,* Science **274**, 1726 (1996).
[7] B. Perman *et al.,* Science **279**, 1946 (1998).
[8] J. Larsson *et al.,* Appl. Phys. A **66**, 587 (1998).
[9] D. A. Reis *et al.,* Phys. Rev. Lett. **86**, 3072 (2001).
[10] S. Techert, F. Schotte, and M. Wulff, Phys. Rev. Lett. **86**, 2030 (2001).
[11] F. Raksi, K. R. Wilson, Z. M. Jiang, A. Ikhlef, C. Y. Cote, and J. C. Kieffer, J. Chem. Phys. **104**, 6066 (1996).
[12] I. V. Tomov, A. Oulianov, P. Chen, and P. M. Rentzepis, J. Phys. Chem. B **103**, 7081 (1999).
[13] C. Rischel *et al.,* Nature (London) **390**, 490 (1997).
[14] A. Rousse *et al.,* Nature (London) **410**, 65 (2001).
[15] C. Rose-Petruck *et al.,* Nature (London) **398**, 310 (1999).
[16] E. Rabinovitch and C. W. Wood, Trans. Faraday Soc. **32**, 547 (1936).
[17] D. E. Smith and C. B. Harris, J. Chem. Phys. **87**, 2709 (1987).
[18] T. J. Chuang, G. W. Hoffman, and K. B. Eisenthal, Chem. Phys. Lett. **25**, 201 (1974).
[19] D. F. Kelley, N. A. Abul-Haj, and D. Jang, J. Chem. Phys. **80**, 4105 (1984).
[20] P. Bado, C. Dupuy, D. Magde, and K. R. Wilson, J. Chem. Phys. **80**, 5531 (1984).
[21] M. Berg, A. L. Harris, and C. B. Harris, Phys. Rev. Lett. **54**, 951 (1985).
[22] A. L. Harris, M. Berg, and C. B. Harris, J. Chem. Phys. **84**, 788 (1986).
[23] J. P. Bergsma, M. H. Coladonato, P. M. Edelsten, J. D. Kahn, K. R. Wilson, and D. R. Fredkin, J. Chem. Phys. **84**, 6151 (1986).
[24] M. Wulff *et al.,* Nucl. Instrum. Methods Phys. Res., Sect. A **398**, 69 (1997).
[25] X. R. Zhu and J. M. Harris, Chem. Phys. **157**, 409 (1991).
[26] B. E. Warren, *X-ray Diffraction* (Dover Publications Inc., New York, 1990).
[27] G. Herzberg, *Molecular Spectra and Molecular Structure, Vol. I. Spectra of Diatomic Molecules* (Krieger Publishing Company, Malabar, 1991).
[28] R. Neutze and R. Wouts, J. Synchrotron. Radiat. **7**, 22 (2000).
[29] R. W. Schoenlein *et al.,* Science **274**, 236 (1996).
[30] R. W. Schoelien *et al.,* Science **287**, 2237 (2000).
[31] A. N. Tarnovsky *et al.,* Chem. Phys. Lett. **312**, 121 (1999).
[32] M. Kolbe, H. Besir, L.-O. Essen, and D. Oesterhelt, Science **288**, 1390 (2000).
[33] M. H. Vos, F. Rappaport, J. C. Lambray, J. Breton, and J. L. Martin, Nature (London) **363**, 320 (1993).
[34] B. H. Wiik, Nucl. Instrum. Methods Phys. Res., Sect. A **398**, 1 (1997).